

Efficacy of a Cancer Vaccine against *ALK*-Rearranged Lung Tumors

Claudia Voena^{1,2}, Matteo Menotti^{1,2}, Cristina Mastini^{1,2}, Filomena Di Giacomo^{1,2}, Dario Livio Longo^{1,3}, Barbara Castella^{1,2}, Maria Elena Boggio Merlo^{1,2}, Chiara Ambrogio⁴, Qi Wang⁵, Valerio Giacomo Minerò^{1,2}, Teresa Poggio^{1,2}, Cinzia Martinengo^{1,2}, Lucia D'Amico^{1,2}, Elena Panizza^{1,2}, Luca Mologni⁶, Federica Cavallo^{1,7}, Fiorella Altruda^{1,7}, Mohit Butaney^{8,9}, Marzia Capelletti^{8,9}, Giorgio Inghirami^{1,2}, Pasi A. Jänne^{8,9,10}, and Roberto Chiarle^{1,2,5}

Abstract

Non-small cell lung cancer (NSCLC) harboring chromosomal rearrangements of the anaplastic lymphoma kinase (*ALK*) gene is treated with *ALK* tyrosine kinase inhibitors (TKI), but the treatment is successful for only a limited amount of time; most patients experience a relapse due to the development of drug resistance. Here, we show that a vaccine against *ALK* induced a strong and specific immune response that both prophylactically and therapeutically impaired the growth of *ALK*-positive lung tumors in mouse models. The *ALK* vaccine was efficacious also in combination with *ALK* TKI

treatment and significantly delayed tumor relapses after TKI suspension. We found that lung tumors containing *ALK* rearrangements induced an immunosuppressive microenvironment, regulating the expression of PD-L1 on the surface of lung tumor cells. High PD-L1 expression reduced *ALK* vaccine efficacy, which could be restored by administration of anti-PD-1 immunotherapy. Thus, combinations of *ALK* vaccine with TKIs and immune checkpoint blockade therapies might represent a powerful strategy for the treatment of *ALK*-driven NSCLC. *Cancer Immunol Res*; 3(12); 1333–43. ©2015 AACR.

Introduction

Lung cancer is the leading cause of cancer-related mortality worldwide. In recent years, the identification of key genetic alterations in non-small cell lung cancer (NSCLC) has prompted the use of rationally targeted therapies, which showed unprecedented clinical benefits (1, 2). Approximately 5% to 6% of NSCLCs have chromosomal rearrangements of the anaplastic lymphoma kinase (*ALK*) gene that generate different chimeric proteins, such as *EML4-ALK*, *TFG-ALK*, and *KIF5b-ALK* (3–5). In all such fusions, constitutively active *ALK* acts as a potent tumor-

igenic driver that activates downstream oncogenic signals, leading to increased cell proliferation and survival (4).

Experimental and clinical data show that *ALK*-rearranged NSCLCs respond to treatment with specific tyrosine kinase inhibitors (TKI), such as crizotinib (6, 7). Despite a high rate of initial response, the development of resistance to crizotinib almost invariably leads to tumor relapse and eventually to the patient's death (8, 9). Next-generation *ALK* TKIs, such as ceritinib and alectinib, have been developed to overcome crizotinib resistance and can further extend survival in crizotinib-resistant patients (10–12). Resistance to *ALK* TKIs is mediated by point mutations of the *ALK* kinase domain, by *ALK* gene amplification, or by activation of other compensatory pathways, so-called bypass tracks, such as *EGFR*, *c-KIT*, *c-MET*, and *IGF-R1* (8, 13–16). Thus, additional therapies to be combined with *ALK* TKIs are needed to further prolong remission or clinical response in NSCLC patients with *ALK* rearrangements.

Immunotherapy aimed at enhancing the immune response against tumor cells shows promising efficacy in a fraction of NSCLC (17, 18). In this context, the *ALK* protein has many features of an ideal tumor oncoantigen that can be exploited to design specific immunotherapies, such as a cancer vaccine. *ALK* is required for tumor survival and growth and expressed minimally in some nervous system cells (4, 19). *ALK* is also antigenic in humans, as lymphoma patients with *ALK* rearrangements mount spontaneous B- and T-cell responses against the *ALK* protein, with measurable antibodies (20), cytotoxic T lymphocytes (CTL), and CD4⁺ T-helper effectors to *ALK* epitopes (21–24). A robust immune response to *ALK* is associated with a decreased risk of relapse in lymphoma patients (25). Our previous *ALK* vaccine in preclinical mouse models of lymphoma containing *ALK* rearrangements induced specific and potent immune responses that provided strong and durable tumor protection (19).

¹Department of Molecular Biotechnology and Health Sciences, University of Torino, Torino, Italy. ²Center for Experimental Research and Medical Studies (CERMS), Città della Salute e della Scienza, Torino, Italy. ³Molecular Imaging Center, University of Torino, Torino, Italy. ⁴Molecular Oncology Program, Centro Nacional de Investigaciones Oncológicas, Madrid, Spain. ⁵Department of Pathology, Children's Hospital Harvard Medical School, Boston, Massachusetts. ⁶Department of Health Sciences, University of Milano-Bicocca, Milano, Italy. ⁷Molecular Biotechnology Center, University of Torino, Torino, Italy. ⁸Department of Medical Oncology, Dana-Farber Cancer Institute, Boston, Massachusetts. ⁹Lowe Center for Thoracic Oncology, Dana-Farber Cancer Institute, Boston, Massachusetts. ¹⁰Belfer Institute for Applied Cancer Science, Dana-Farber Cancer Institute, Boston, Massachusetts.

Note: Supplementary data for this article are available at Cancer Immunology Research Online (<http://cancerimmunolres.aacrjournals.org/>).

M. Menotti and C. Mastini contributed equally to this article.

Corresponding Author: Roberto Chiarle, Children's Hospital Boston and Harvard Medical School, 300 Longwood Avenue, Boston, MA 02115. Phone: 617-919-2662; Fax: 617-730-0148; E-mail: roberto.chiarle@childrens.harvard.edu

doi: 10.1158/2326-6066.CIR-15-0089

©2015 American Association for Cancer Research.

Voena et al.

In the present study we test the efficacy of ALK vaccination in lung cancer. Grafted or primary mouse models of ALK-positive lung tumors showed that an ALK vaccine elicited a strong, ALK-specific CTL response in both mouse models, efficiently blocking tumor growth.

Materials and Methods

Cell lines and reagents

Human ALK-rearranged NSCLC cell lines H2228 (variant 3, E6; A20), DFCI032, and H3122 (variant 1, E13;A20) were obtained from the ATCC collection and were passaged for fewer than 6 months after receipt and resuscitation. These cell lines were further internally tested for the presence of EML-ALK rearrangement. The murine ASB-XIV cell line was purchased from Cell Lines Service (CLS) and was passaged for fewer than 6 months after receipt and resuscitation.

The ALKTKI NVP-TAE684 was purchased from Axon Medchem and crizotinib (PF-02341066) was kindly gifted by Pfizer.

Mice

Strains of mice used in this study include K-Ras^{LSL/G12V} and Tg EGFR^{L858R}, as previously published (26, 27), and BALB/c mice (Charles River). Mice were handled and treated in accordance with European Community guidelines.

Generation of ALK transgenic mice

A cDNA fragment encoding EML4-ALK (variant 1, E13;A20) or TFG-ALK was ligated to the human SP-C promoter as well as to a polyadenylation signals (Supplementary Fig. S1A). The expression cassette was injected into pronuclear-stage embryos of FVB/N mice. The presence of the transgene was examined by PCR analysis with DNA from the tail of founder animals. Mice were handled and treated in accordance with European Community guidelines. Methods are further described in Supplementary Materials and Methods.

DNA vaccination and *in vivo* cytotoxicity assay

For DNA vaccination, 50 µg of pDEST or pDEST-ALK plasmids were used as previously described (19). The *in vivo* cytotoxicity assay was previously reported (19).

Antibody dosing for *in vivo* treatment

For CD4⁺ and CD8⁺ cell depletion, anti-CD4 (clone GK1.5) and anti-CD8 (clone 2.43) antibodies were purchased from BioXcell. For depletion, mice were injected i.p. with 100 µg of anti-CD4 or anti-CD8 at days -1, +5, +15, and +25.

For PD-1 blockade, anti-PD-1 (clone J43) and control anti-hamster polyclonal IgG for the *in vivo* experiments were purchased from BioXcell. Mice received 200 µg of each anti-PD-1 and anti-PD-L1 or 200 µg of anti-hamster IgG i.p. every 3 days for a total of 5 injections.

Magnetic resonance imaging

Magnetic resonance images (MRI) were acquired on a Bruker Avance 300 spectrometer operating at 7 T and equipped with a microimaging probe (Bruker Bio-Spin), as described in Supplementary Materials and Methods.

Histology and immunohistochemistry

For histologic evaluation, tissue samples were fixed in formalin, embedded in paraffin, stained, and visualized as previously

described (19). T lymphocytes and regulatory T cells (Tregs) were quantified by measuring the number of CD3⁺, CD8⁺, CD4⁺, and Foxp3⁺ cells, respectively, among the total tumor cells.

Intratumoral cell characterization

For flow cytometry analysis, lung cell infiltrate was obtained using the Lung Dissociation Kit (Miltenyi Biotec) following the manufacturer's instructions. Cells were resuspended in phosphate buffer and stained with antibodies described in Supplementary Materials and Methods.

Statistical methods

Kaplan–Meier analyses for survival curves were performed with GraphPad Prism 5, and *P* values were determined with a log-rank Mantel–Cox test. Paired data were compared with the Student *t* test. *P* values of <0.05 were considered to be significant. Unless otherwise noted, data are presented as mean ± SEM.

Results

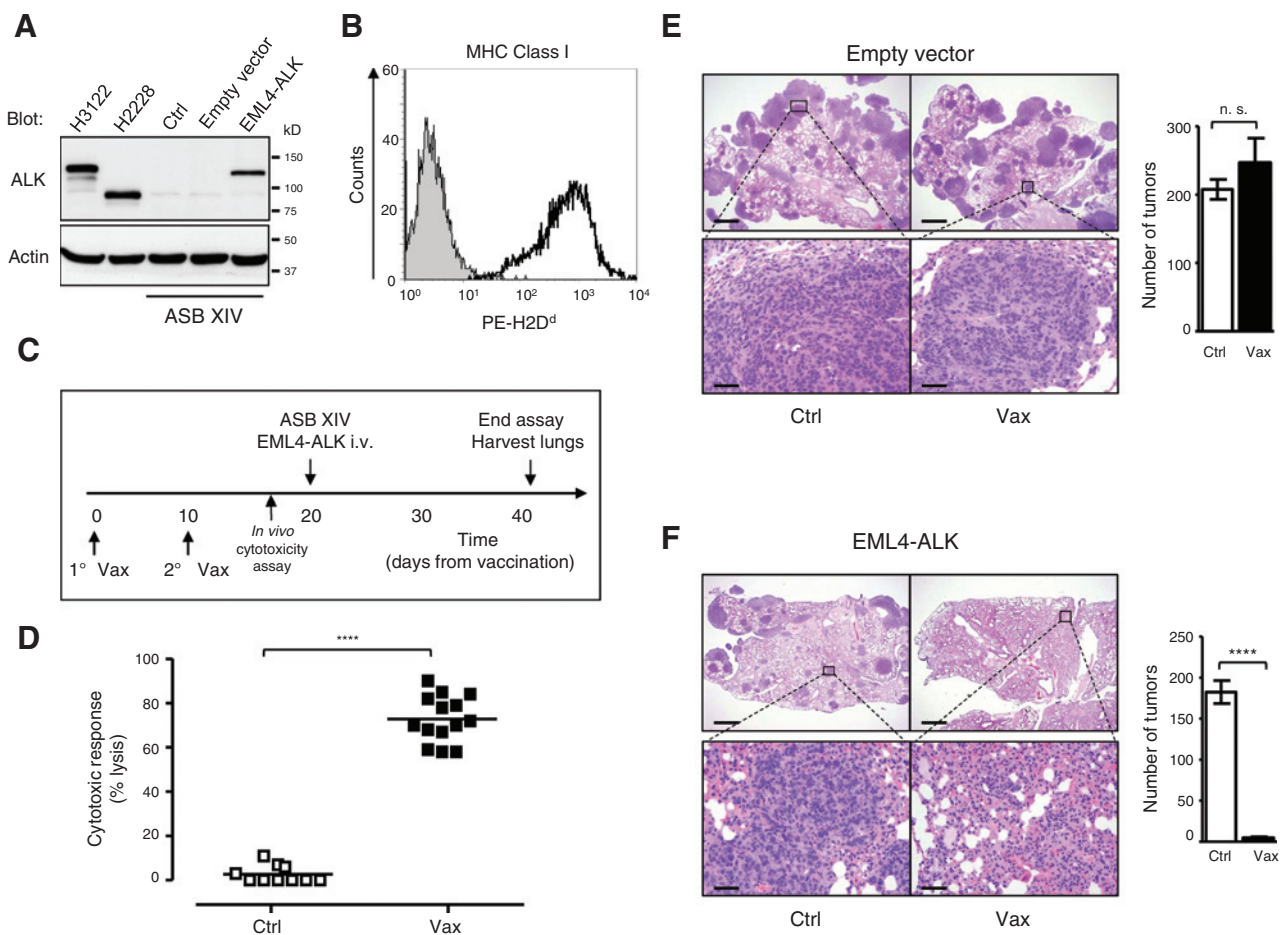
ALK vaccination elicits a specific cytotoxic response and prevents tumor growth in an orthotopic model of ALK-positive lung cancer

To test the efficacy of the ALK vaccine against lung cancer, we developed an orthotopic mouse model of ALK-positive lung cancer by ectopic expression of EML4-ALK in the syngeneic BALB/c murine lung cancer cell line ASB-XIV. We transduced ASB-XIV cells with a retroviral vector containing the EML4-ALK cDNA (variant 1) and GFP as a reporter. Protein expression in transduced ASB-XIV cells was comparable with EML4-ALK expression in human ALK-rearranged NSCLC cells (variant 1 in H3122 and 3 in H2228; Fig. 1A). ASB-XIV cells express MHC class I and thus are suitable for tumor immune studies (Fig. 1B). Within 3 weeks after i.v. injection of 5×10^5 ASB-XIV cells into the mouse tail vein, tumor nodules were detected in both lungs (Fig. 1E and F). We vaccinated BALB/c mice with a DNA plasmid coding for the intracytoplasmic domain of ALK (ref. 19; Fig. 1C).

ALK vaccine induced a strong ALK-specific immune response as measured by an *in vivo* cytotoxic assay (ref. 19; Fig. 1D). Ten days after the second vaccination, we injected EML4-ALK or GFP ASB-XIV cells. GFP ASB-XIV cells gave equal numbers of tumors in mice vaccinated with either a control or the ALK plasmid (Fig. 1E). In contrast, tumors of EML4-ALK ASB-XIV cells had impaired growth in ALK-vaccinated mice (Fig. 1F). Thus, ALK vaccination induced an ALK-specific immune response that efficiently prevented the growth of ALK-positive lung tumors.

ALK vaccination delays tumor growth and increases the overall survival of EML4-ALK-rearranged NSCLC Tg mice

To test the efficacy of the ALK vaccine as a therapy for primary lung tumors, we generated two transgenic (Tg) mouse models of ALK-driven lung cancers. Two rearrangements of ALK (EML4-ALK, variant 1, or TFG-ALK) were expressed under the human lung-specific surfactant protein-C (SP-C) promoter (Supplementary Fig. S1A), because human ALK-rearranged NSCLCs are often SP-C positive (28), and the expression of EML4-ALK by the SP-C promoter can induce efficient lung tumor formation in mice (29). Both transgenic mouse models expressed the ALK fusion selectively in lung epithelial cells, in amounts comparable with human NSCLC with rearranged ALK (Supplementary Fig. S1B–S1D), and rapidly developed multifocal

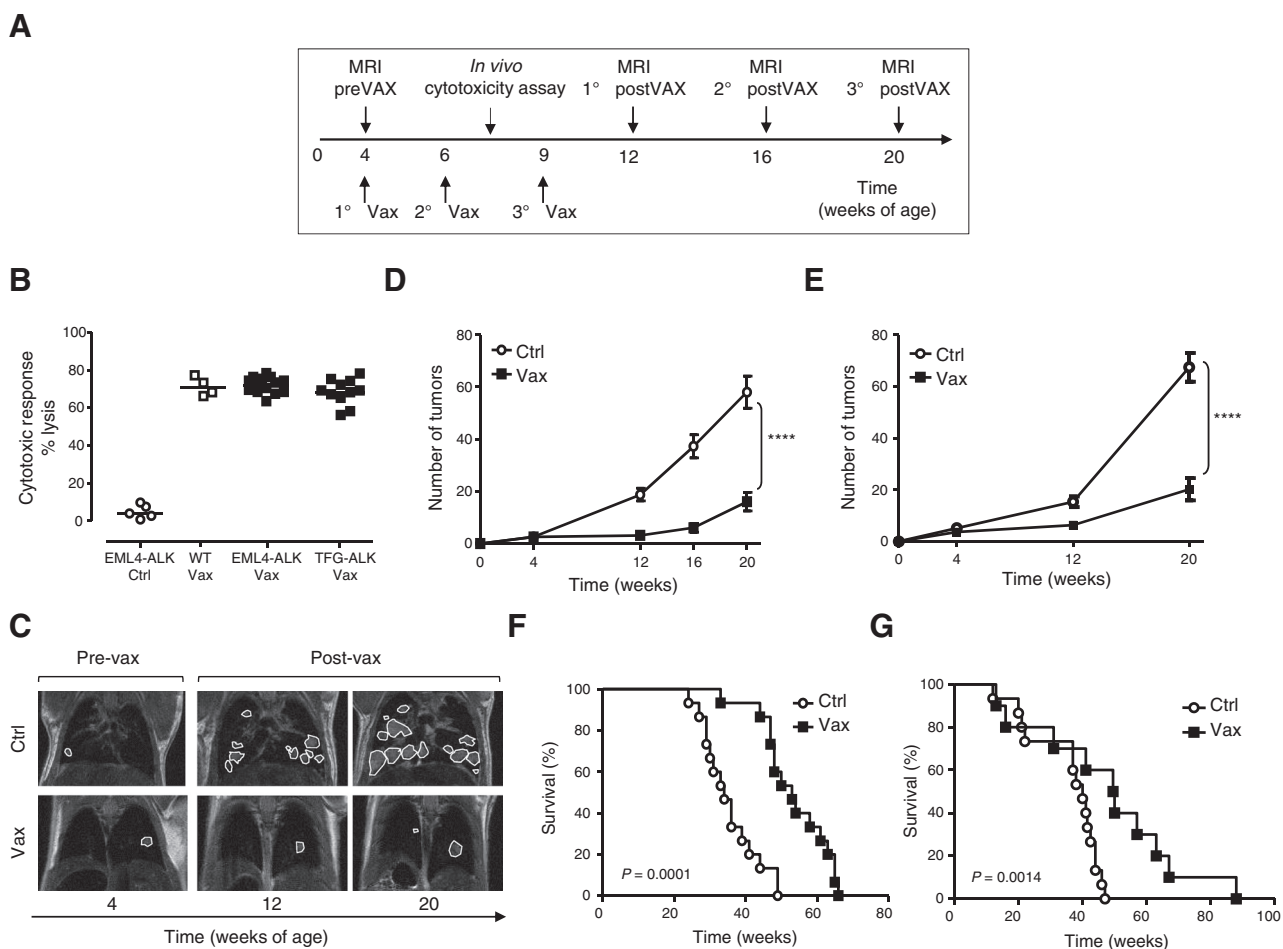
**Figure 1.**

Prophylactic ALK vaccine prevents the growth of ALK-positive lung tumors in an orthotopic model. A, EML4-ALK expression in ASB-XIV-infected cells and in human EML4-ALK NSCLC cell lines (H3122 and H2228) was evaluated by immunoblotting with the indicated antibodies. B, analysis of the MHC class I (PE-H2D^d Ab) antigen expression on ASB-XIV cells by flow cytometry. C, schematic representation of ALK vaccination protocol in BALB/c mice. Control mice were vaccinated with empty pDEST (Ctrl), and ALK-vaccinated mice were vaccinated with pDEST-ALK (Vax). D, cytotoxic activity in ALK-vaccinated mice evaluated by an *in vivo* cytotoxicity assay. Horizontal bars represent mean. E and F, representative hematoxylin and eosin (H&E) sections of lungs injected with GFP-ASB-XIV cells (E) or EML4-ALK ASB-XIV cells (F). Histograms represent the number of tumors in control (Ctrl; $n = 3$ mice) and ALK-vaccinated mice (Vax; $n = 3$ mice). Scale bars, 1 mm (top) and 50 μ m (bottom). The total number of tumors was counted in the whole lung of each mouse. Data are represented from three independent experiments as mean (\pm SEM). ****, $P < 0.0001$. n.s., not statistically significant.

ALK-positive tumors few weeks after birth, with 100% penetrance (Supplementary Fig. S1E and S1F). Tumors were mainly well-differentiated adenocarcinoma growing as papillary, acinar, or more solid carcinoma (30). Ki-67 immunostaining showed that these tumors had a proliferation rate of $10.5\% \pm 1.4\%$ for EML4-ALK and $8.5\% \pm 1.9\%$ for TFG-ALK (Supplementary Fig. S1G). At 4 weeks of age, a few tumor nodules in both types of ALK mice (Supplementary Fig. S1H and S1I, left) were detected by MRI. Existing nodules rapidly expanded in volume and new nodules appeared in the lungs over time (Supplementary Fig. S1H and S1I, central and right plots). No tumor metastases were detected by examination of other organs with MRI or histology in ALK mice at any age, consistent with other constitutive or ALK-inducible mice (29, 31). Both EML4-ALK and TFG-ALK mice died within 50 weeks, with a mean survival of 33.25 weeks for EML4-ALK mice and 37 weeks for TFG-ALK mice (Supplementary Fig. S1L).

To test the efficacy of the ALK vaccine, we screened ALK mice by MRI to stratify them according to their tumor burden. ALK mice were vaccinated at 4 weeks of age, when tumors were detectable in the lungs (Supplementary Fig. S1H and S1I), according to the protocol in Fig. 2A. The ALK vaccine generated strong ALK-specific cytotoxic activity in both ALK models, comparable with wild-type (WT) littermates (Fig. 2B). In EML4-ALK mice, the average number of tumors detected in control mice was 58 ± 6.0 by week 20, whereas ALK-vaccinated mice had only 16 ± 3.5 at the same time point (Fig. 2C and D). Similar results were observed in TFG-ALK mice at 20 weeks of age (67 ± 6.0 nodules in control mice compared with 20 ± 3.5 nodules in vaccinated mice; Fig. 2E and Supplementary Fig. S2A). Correspondingly, the overall tumor burden calculated in terms of tumor volumes by serial MRI was significantly lower in ALK-vaccinated mice than in control mice (Supplementary Fig. S2B and S2C). Survival of ALK-vaccinated mice was

Voena et al.

**Figure 2.**

Therapeutic ALK vaccine delays tumor progression in *ALK*-rearranged NSCLC. A, ALK vaccination protocol in *ALK* Tg mice. B, cytotoxic activity in control mice (○) and ALK-vaccinated (Vax) WT mice (□) or Tg mice (■). Horizontal bars represent mean. C, representative coronal MRI sections of lungs from EML4-*ALK* mice. D and E, number of tumors in control (Ctrl) and ALK-vaccinated (Vax) mice as measured by MRI at the indicated time points. EML4-*ALK* mice (D, Ctrl = 24 mice; Vax = 26 mice) from three independent experiments. TFG-*ALK* mice (E, Ctrl = 5 mice; Vax = 9 mice) from two independent experiments. The average number of tumors for each cohort (\pm SEM) is displayed. F and G, overall survival by Kaplan-Meier curves in EML4-*ALK* mice (F) and TFG-*ALK* mice (G). ****, $P < 0.0001$.

significantly extended by at least 18 weeks in EML4-*ALK* and by 12 weeks in TFG-*ALK* mice (Fig. 2F and G). The ALK vaccine was still efficacious against larger tumors in older mice (Supplementary Fig. S2D). Thus, ALK-DNA vaccination was a potent controller of growth of primary *ALK*-rearranged lung tumors.

ALK-DNA vaccination increases the number of intratumoral T cells and requires CD8⁺ T lymphocytes

Next, we examined how the ALK vaccine shaped the intratumoral immune infiltrate. The ALK vaccine increased the number of intratumoral T cells in both EML4-*ALK* and TFG-*ALK* mice, which was associated with a reduced tumor size (Fig. 3A and B). Both CD4⁺ and CD8⁺ T cells were significantly increased in ALK-vaccinated mice (Fig. 3C). In ALK-vaccinated mice, tumor-infiltrating T cells had a significantly higher CD8⁺:CD4⁺ ratio compared with controls, due to the DNA vaccine preferentially stimulating a CD8⁺ T-cell immune response (Fig. 3C; ref. 32). We also observed an increase in intratumoral Tregs (Fig. 3D and E), suggesting that the ALK vaccine induces both T_{eff} cells and Tregs,

as described for other tumor vaccines (33). Nonetheless, the ratio of CD8⁺:Foxp3⁺ was higher in vaccinated mice than in control mice (Fig. 3E).

To confirm that the ALK vaccine required T_{eff} for its antitumor functions, we used repeated injections of antibodies specific for CD4⁺ and CD8⁺ T cells to deplete them in the orthotopic model based on EML4-*ALK* ASB-XIV cells (Fig. 3F). The depletion of CD8⁺ T cells, but not CD4⁺ T cells, significantly reduced the ALK vaccine efficacy (Fig. 3G and H). Therefore, in mice bearing ALK-positive tumors, ALK vaccination elicited a cytotoxic response largely mediated by CD8⁺ T cells. However, in mice depleted of CD8⁺ T cells, the vaccine still appeared to retain some activity, suggesting that other factors may be involved in the immune response elicited by the vaccine.

Immunosuppressive lung microenvironment in ALK-rearranged lung cancer

We showed that the ALK vaccine stimulates a potent immune response against *ALK*-rearranged lung tumors. However, the

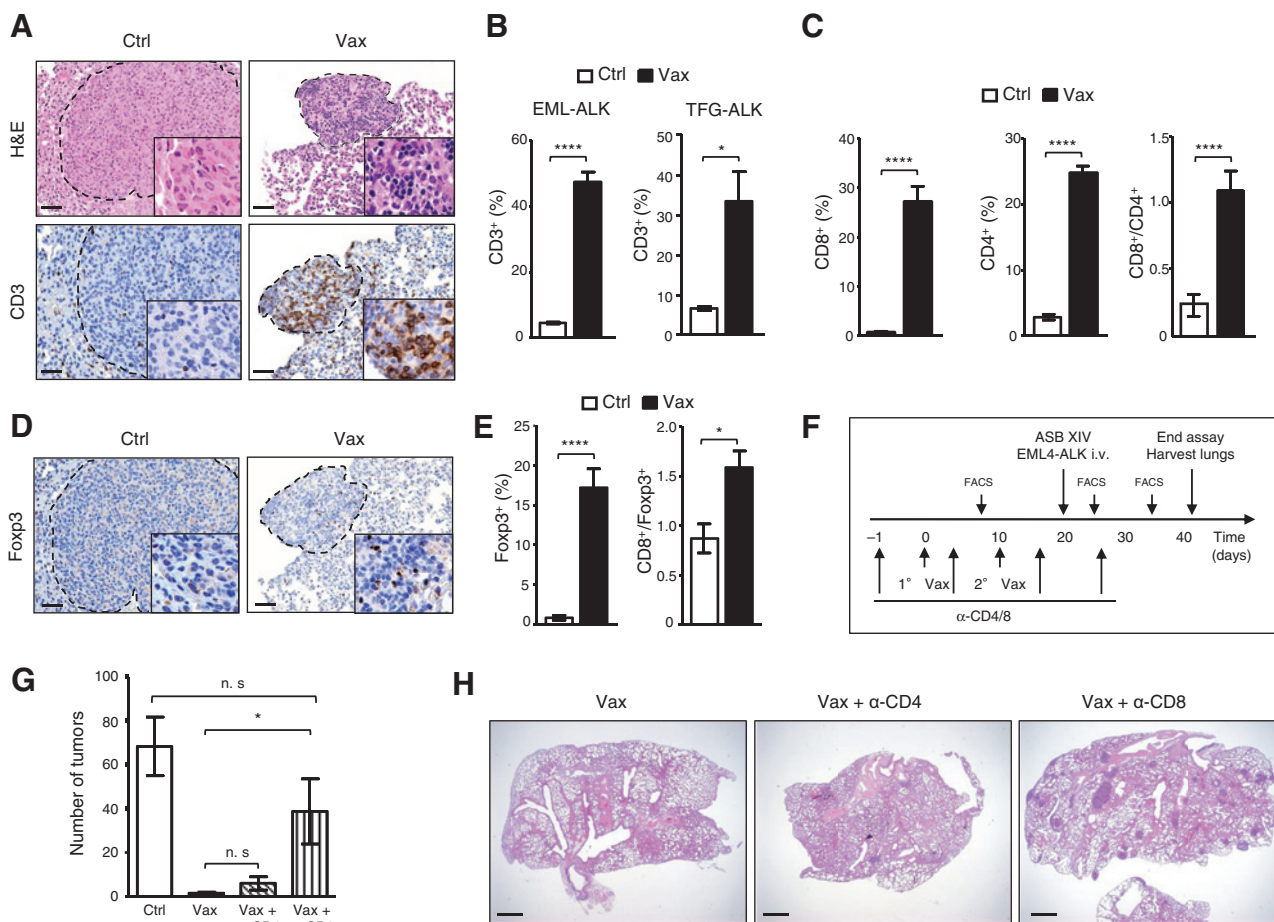


Figure 3.

ALK vaccine increases the number of intratumoral T lymphocytes and depends on cytotoxic CD8⁺ T cells. A, representative hematoxylin and eosin (H&E) and immunostaining with anti-CD3 antibody of lung sections from control (Ctrl) and ALK-vaccinated (Vax) EML4-ALK mice. Scale bars, 100 μ m. B, histograms represent the percentage of CD3⁺ cells infiltrating the tumors in control (Ctrl) and ALK-vaccinated mice (Vax) in EML4-ALK (left) and in TFG-ALK (right) mice at 12 weeks of age. C, histograms represent the mean percentages of CD8⁺ and CD4⁺ T cells infiltrating the tumors and the CD8⁺/CD4⁺ ratio in control and vaccinated EML4-ALK mice at 12 weeks of age. D, representative immunostaining with anti-Fopx3 antibody of lung sections from EML4-ALK control (Ctrl) and ALK-vaccinated (Vax) mice (left). Scale bars, 100 μ m. E, mean percentages of intratumoral Tregs (Fopx3⁺ cells; left) and CD8⁺/Fopx3⁺ cell ratio (right) in control and vaccinated EML4-ALK mice. F, schematic representation of the vaccination protocol in combination with CD4⁺ or CD8⁺ cell depletion. G, mean lung tumor numbers ($n = 5$ mice for each group). Data are from two independent experiments. H, representative lung sections of ALK-vaccinated mice in combination with CD4⁺ cell depletion or CD8⁺ cell depletion. Scale bars, 1 mm. Data are represented as mean (\pm SEM). *, $P < 0.05$; ****, $P < 0.0001$. α -CD4, anti-CD4; α -CD8, anti-CD8; n.s., not statistically significant.

ALK vaccine did not cure the mice, which died after a delay in tumor growth (Fig. 2). Because ALK was still expressed in late tumors, we asked whether the efficacy of the ALK vaccine would diminish over time due to an immunosuppressive microenvironment that progressively develops in lung tumors with ALK rearrangements. Indeed, oncogenic activation of EGFR in lung cancers induces an immunosuppressive lung microenvironment by induction of PD-L1 expression on the surface of tumor lung epithelial cells (34).

First, we better characterized the immune infiltrate in mice bearing ALK lung tumors and observed that overall the percentage of B and T lymphocytes, natural killer (NK) cells, and granulocytes was comparable between WT and EML4-ALK mice (Supplementary Fig. S3A–S3D). However, T cells in tumor-bearing EML4-ALK mice displayed a significantly higher expression of PD-1 on both CD4⁺ and CD8⁺ T cells (Fig. 4A and Supplementary Fig. S3E), and PD-1⁺CD3⁺ T cells also expressed other T-cell-inhibitory mole-

cules such as LAG-3 and TIM-3 in higher amounts (Supplementary Fig. S3E). In addition, Fopx3⁺ Tregs were also increased in EML4-ALK mice over time (Supplementary Fig. S3F). These data suggest that tumor lungs bearing EML4-ALK develop an immunosuppressive microenvironment reminiscent of that seen in EGFR-driven lung cancer models (34).

We also characterized the immune microenvironment in human ALK-rearranged NSCLC. NSCLC patients with ALK rearrangements had lower percentages of CD3⁺, CD4⁺, and CD8⁺ intratumoral T-cell infiltrate than EGFR-mutated NSCLC (Fig. 4B). These findings were further extended by interrogating gene-expression profiling data from larger series of human NSCLC with different oncogenic mutations. By gene set enrichment analysis, we found lower expression of tumor-infiltrating T-cell-related molecules in EML4-ALK NSCLC compared with EGFR-mutated, K-RAS-mutated, or ALK/RAS/EGFR-nonmutated NSCLC (Fig. 4C). In particular, in ALK-rearranged tumors, we

Voena et al.

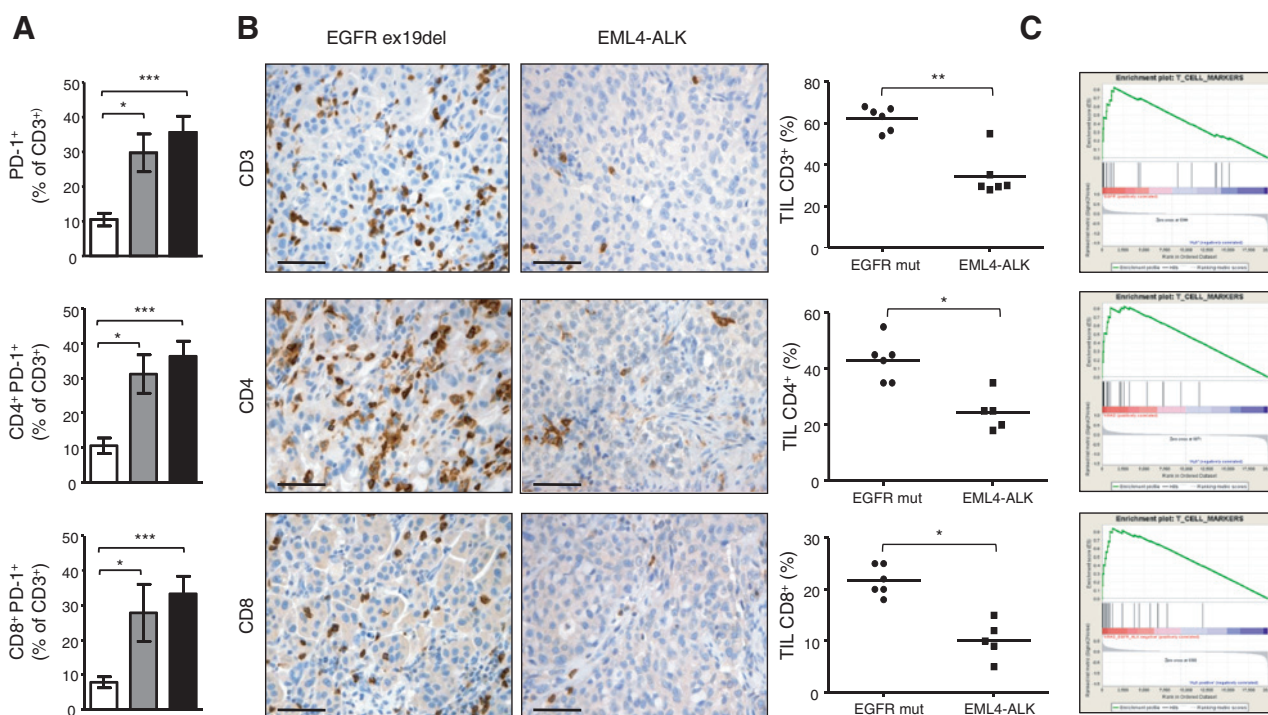


Figure 4. ALK induces an immunosuppressive microenvironment in *ALK*-rearranged NSCLC. A, lung immune infiltrates were stained with antibodies to CD3, CD4, CD8, and PD-1 and analyzed by flow cytometry. Histograms show the mean percentage for each indicated population in WT mice (□, $n = 5$ mice), 12-week-old EML4-ALK mice (■, $n = 5$ mice), and 16-week-old EML4-ALK mice (■, $n = 9$ mice). B, immunohistochemistry for CD3, CD4, and CD8 on a representative mutated EGFR (ex19del) patient (left plots) and a representative EML4-ALK-positive NSCLC case (right plots). Scale bars, 100 μ m. Graphs show the percentages of CD3⁺, CD4⁺, and CD8⁺ cells in EML4-ALK-positive NSCLC versus EGFR-mutated patients. Horizontal bars represent mean. C, gene set enrichment analysis for T-cell markers based on gene expression profiling of human EML4-ALK NSCLC versus EGFR-mutated NSCLC (L858R or EGFR-Del19; FDR q-value: 0.008, top plot) or versus K-RAS-mutated NSCLC (FDR q-value: 0.001, central plot) or versus K-RAS/EGFR/ALK-negative NSCLC (FDR q-value: 0.00046, bottom plot). *, $P < 0.05$; **, $P < 0.005$; ***, $P < 0.0005$.

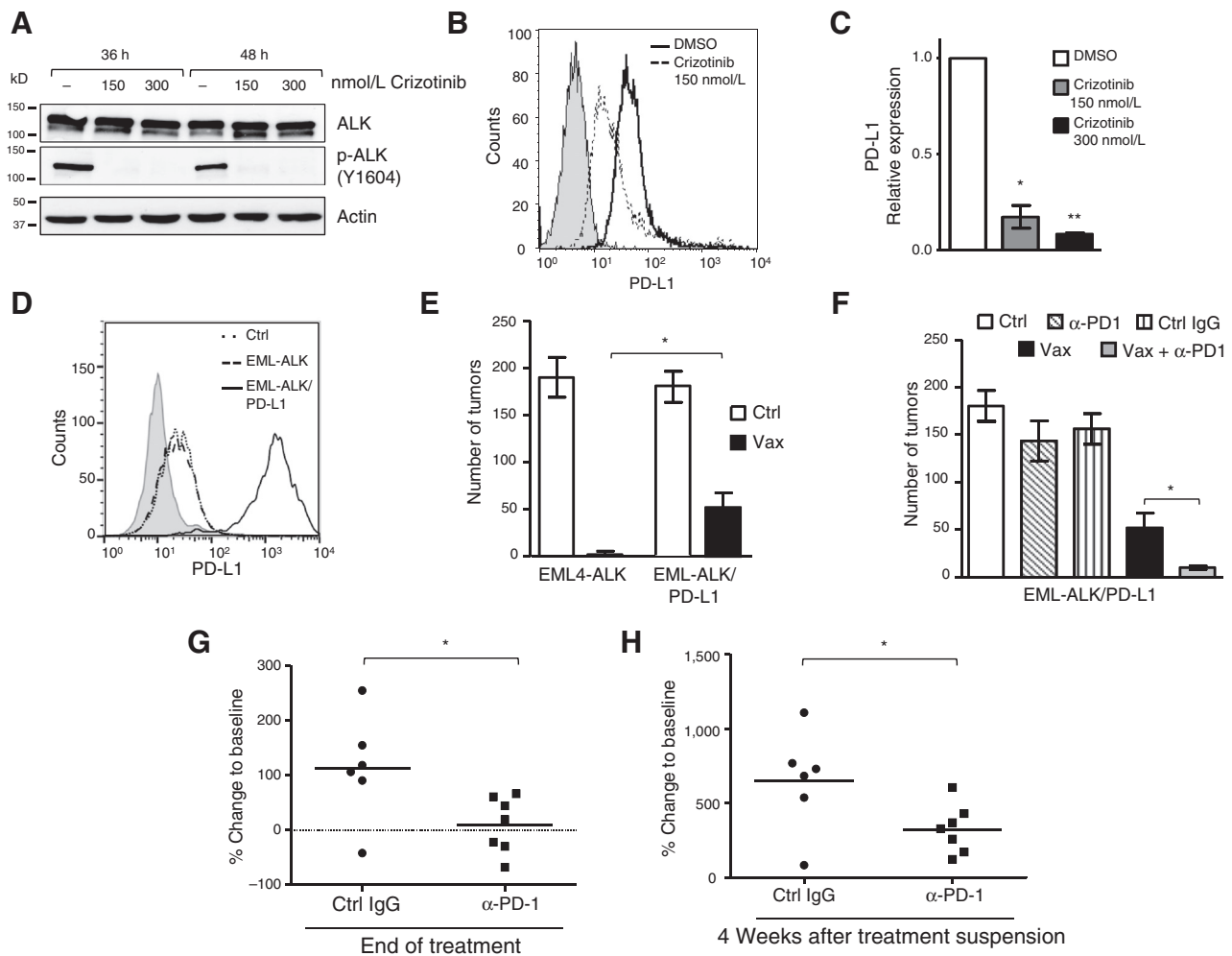
observed significant depletion of T-cell receptor (TCR)-related molecules, such as TCR β chain, CD3 δ , CD3 γ , CD3 ζ , and *Lck*, of the T-cell costimulatory molecules ICOS and CD28, as well as of CD80 and CTLA-4 (Supplementary Fig. S4A–S4D).

Blockade of the PD-1/PD-L1 pathway restores ALK vaccine efficacy against tumor cells with high levels of PD-L1

We asked whether oncogenic ALK could also regulate PD-L1 expression on lung tumors. Tumors derived from EML4-ALK mice had higher levels of PD-L1 expression than tumors originating in mice carrying other NSCLC recurrent mutations, such as the K-Ras^{G12V} (26) and EGFR^{L858R} (27) mice (Supplementary Fig. S5A). Next, we analyzed PD-L1 expression by flow cytometry and showed that tumor epithelial cells (CD45⁻/EpCAM⁺) and associated hematopoietic cells (CD45⁺) in EML4-ALK mice expressed PD-L1 (Supplementary Fig. S5B). To determine whether ALK oncogenic activity directly controlled PD-L1 expression in NSCLC, we treated three *ALK*-rearranged NSCLC cell lines (H3122, H2228, and DFCI032) with crizotinib to inhibit ALK activity (Fig. 5A and Supplementary Fig. S5C). Expression of PD-L1 was detectable in all *ALK*-rearranged cell lines tested and was reduced upon ALK inhibition in all three cell lines (Fig. 5B and Supplementary Fig. S5D). Consistently, PD-L1 mRNA was also downregulated (Fig. 5C and Supplementary Fig. S5E). To further confirm that PD-L1 expression was driven by ALK activity, and to

exclude the possibility that PD-L1 downregulation was mediated by crizotinib inhibition of MET, ROS1, or other off-targets, we knocked down EML4-ALK by a doxycycline-inducible shRNA system (16). Again, PD-L1 expression was downregulated upon EML4-ALK knockdown (Supplementary Fig. S5F and S5G). We conclude that in *ALK*-rearranged NSCLC, PD-L1 mRNA and protein were regulated by ALK activity. Another group has recently confirmed these findings (35).

The expression of PD-L1 of the surface of tumor cells impairs antitumor activity of the immune system (36). We investigated whether the efficacy of the ALK vaccine could be diminished by the expression of PD-L1 on the surface of the target lung tumor cells. EML4-ALK mice express moderate, but detectable PD-L1, and we observed similar intensity of expression by flow cytometry in EML4-ALK ASB-XIV (Fig. 5D). We reasoned that ALK vaccine efficacy could be hampered when target tumor cells express more PD-L1. We engineered EML4-ALK ASB-XIV cells to express more PD-L1 than parental cells by transduction with a lentivirus containing a murine PD-L1 construct (Fig. 5D). Vaccinated mice were injected with control EML4-ALK ASB-XIV cells or EML4-ALK ASB-XIV cells expressing high PD-L1. In the presence of high PD-L1 expression, the ALK vaccine was less effective in preventing lung tumor growth (Fig. 5E), suggesting that the function of ALK-specific T_{eff} cells was modulated by the amount of PD-L1 on the surface of target lung tumor cells.

**Figure 5.**

Blockade of the PD-1/PD-L1 pathway restores the efficacy of the ALK vaccine against cells expressing high PD-L1. A, Western blot of H3122 cells treated with different crizotinib concentrations and collected at the indicated time points. Membranes were blotted with the indicated antibodies. B, PD-L1 protein expression was evaluated by flow cytometry in H3122 cells treated with 150 nmol/L of crizotinib for 24 hours. C, PD-L1 mRNA expression was evaluated by qRT-PCR in crizotinib-treated cells. D, PD-L1 expression was evaluated by flow cytometry in ASB-XIV cells (Ctrl), EML4-ALK ASB-XIV (EML-ALK), and in EML4-ALK ASB-XIV transduced with PD-L1 (EML4-ALK/PD-L1). E, mean tumor numbers in lungs from mice injected with the indicated ASB-XIV cells ($n = 5$ mice for each group). F, mean tumor numbers in lungs from mice with the indicated treatments ($n = 6-8$ mice for each group). Data are represented as mean (\pm SEM). G and H, quantification of volume changes compared with baseline tumors in ALK mice treated with control IgG ($n = 6$ mice) or anti-PD-1 antibody ($n = 7$ mice) at the end of treatment (G) and 4 weeks after treatment suspension (H). Horizontal bars represent mean. Data are from two independent experiments. *, $P < 0.05$; **, $P < 0.005$. α -PD-1, anti-PD-1.

To test whether administration of antibody to PD-1 could restore a full efficacy of the ALK vaccine, we treated mice with anti-PD-1 or control IgG (Supplementary Fig. S6A). The treatment with anti-PD-1 alone, as well as control IgG, did not have significant effect on tumor growth and mice developed tumors comparable with controls. In contrast, anti-PD-1 treatment almost completely restored the efficacy of the ALK vaccine (Fig. 5F). These results are consistent with findings that immune checkpoint therapy restores an adaptive immune response best in patients with high PD-L1 expression (37, 38).

To show that blockade of the PD-L1/PD-1 immune checkpoint was effective with physiologic expression of PD-L1, we tested anti-PD-1 treatment in EML4-ALK mice (Supplementary Fig. S6B). We observed a stabilization of tumors immediately at the

end of treatment (Fig. 5G) followed by a slower growth rate as compared with control mice (Fig. 5H). These data suggest that immune checkpoint blockade therapy could be efficacious in the physiologic tumor microenvironment of ALK-rearranged lung tumors.

ALK vaccination is effective in combination with ALK TKIs

Crizotinib treatment of NSCLC patients with ALK rearrangements has had success in clinical trials, supporting the use of ALK TKIs as main therapy for NSCLC (39). A combination of ALK TKIs with the ALK vaccine could be an attractive therapeutic possibility for NSCLC patients. In this context, ALK TKIs could reduce the tumor burden to facilitate the activity of the ALK vaccine. We tested this combination in our ALK mouse

Voena et al.

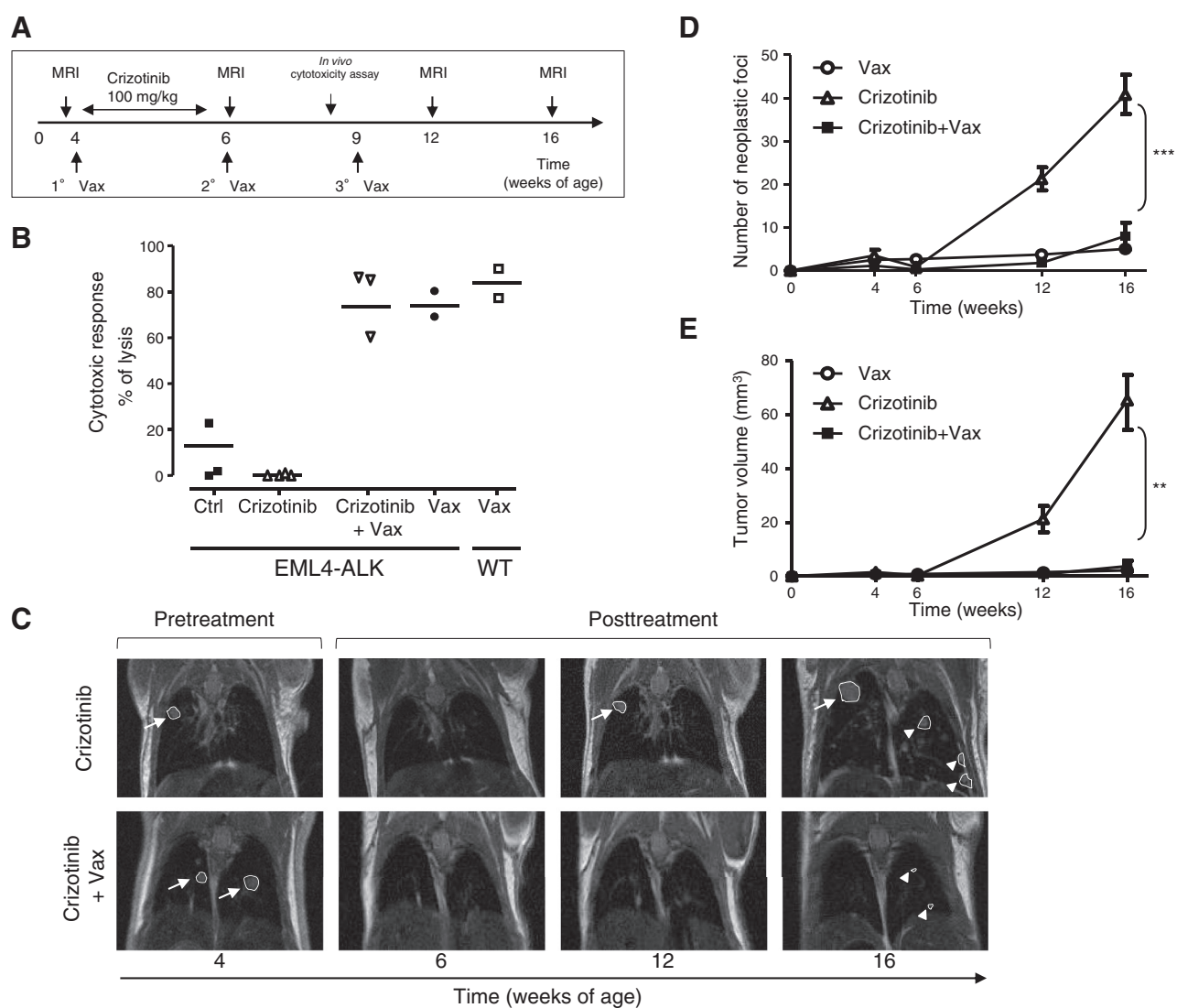


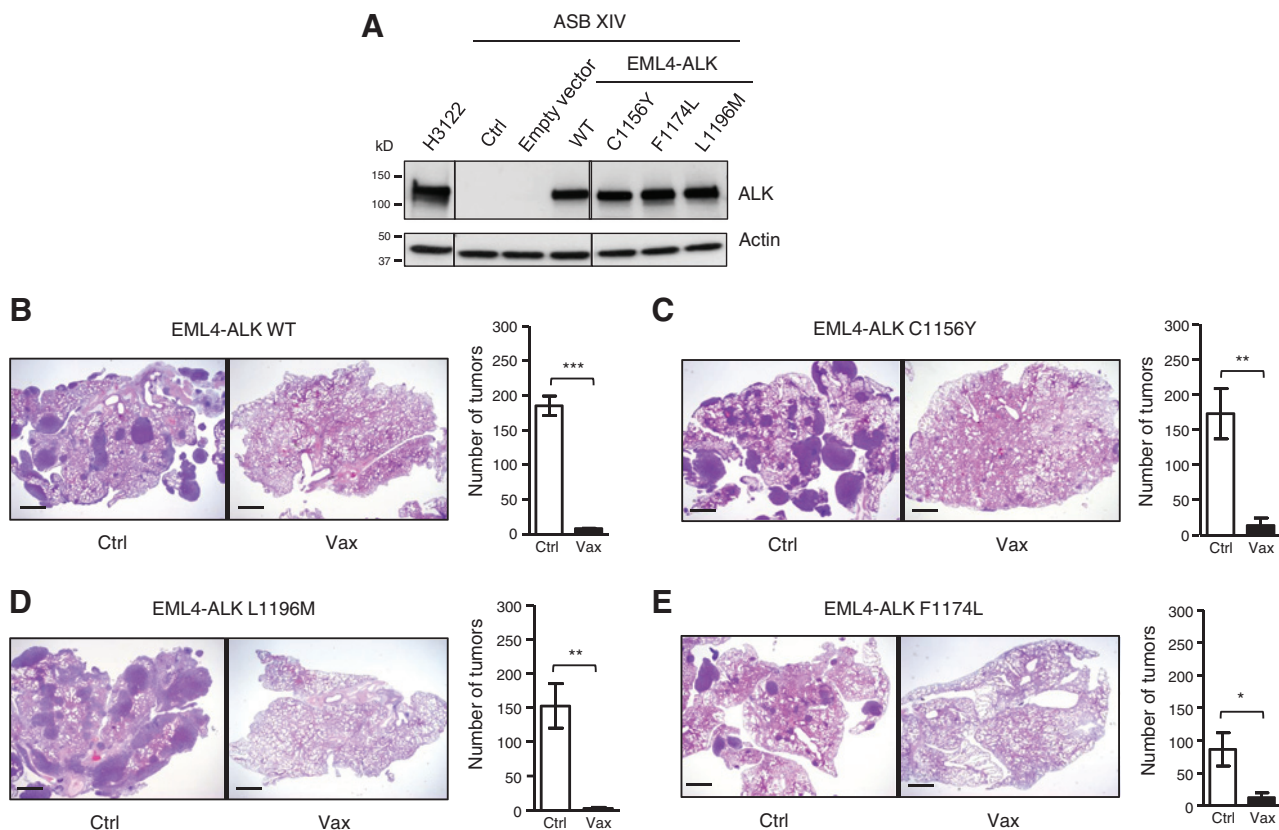
Figure 6. ALK vaccine is efficacious in combination with crizotinib treatment. A, schematic representation of the ALK vaccination combined with crizotinib treatment in EML4-ALK mice. B, cytotoxic activity in ALK-vaccinated mice in combination with crizotinib. Horizontal bars represent mean. C, representative MRI of crizotinib-treated mice and crizotinib-treated plus vaccinated mice. Arrows indicate tumor recurrence in the same position. Arrowheads indicate new tumors. D and E, the number of tumors (D) and the tumor volume (E) were measured by MRI analysis at the indicated time points. Data are from two independent experiments. Data are represented as mean (\pm SEM). **, $P < 0.005$; ***, $P < 0.0005$.

models. ALK mice were treated with crizotinib (PF-02341066) for 2 weeks (100 mg/kg) and concurrently vaccinated with the ALK or control vaccine (Fig. 6A). The immune response elicited by the vaccine was not affected by administration of crizotinib, as an equally strong ALK-specific cytotoxic immune response *in vivo* was also detected in ALK-vaccinated mice treated with crizotinib (Fig. 6B). As expected, treatment with crizotinib induced the regression of tumors in both groups within 2 weeks (Fig. 6C, left and central plots; 6D). At 6 weeks from treatment suspension, tumors relapsed at the same sites in crizotinib-treated mice (Fig. 6C, top right plots), whereas the combination of crizotinib and ALK vaccine delayed tumor recurrence (Fig. 6C, bottom right plots). Indeed, mice treated with crizotinib showed relapses and new tumors 10 weeks after

treatment suspension, whereas in ALK-vaccinated mice, relapses and new tumors were less numerous and significantly smaller (Fig. 6D and E). Similar results were obtained when EML4-ALK mice were vaccinated during treatment with TAE684 (25 mg/kg; Supplementary Fig. S7A–S7C). Thus, the ALK vaccine might be efficiently combined with ALK TKI treatment to delay tumor relapse after crizotinib suspension.

ALK vaccination prevents growth of tumors expressing crizotinib-resistant ALK mutations

Human NSCLC patients treated with ALK TKI almost invariably develop resistance. L1196M, C1156Y, and F1174L are common ALK mutations found in patients relapsing under treatment with crizotinib (8, 12, 13). Point mutations in the ALK kinase

**Figure 7.**

ALK vaccine is effective in tumors with crizotinib-resistant EML4-ALK mutants. A, Western blot shows the expression of EML4-ALK WT or the EML4-ALK mutants (C1156Y, F1174L, and L1196M) in ASB-XIV-infected cells and in human *ALK*-rearranged NSCLC cell line (H3122). The lines between the blots indicate cut lanes on the same gel. B-E, representative hematoxylin and eosin sections of the lungs of control (Ctrl) and ALK-vaccinated (Vax) mice at day 21 after i.v. injection of ASB-XIV cells infected with a GFP plasmid expressing EML4-ALK WT (B) or the EML4-ALK mutants C1156Y (C), L1196M (D), or F1174L (E). Histograms represent the number of tumors in control (Ctrl; $n = 3$ mice for each EML4-ALK construct) and ALK-vaccinated mice (Vax; $n = 3$ mice for each EML4-ALK construct). Scale bars, 1 mm. Data are from two independent experiments. Data are represented as mean (\pm SEM). *, $P < 0.05$; **, $P < 0.005$; ***, $P < 0.0005$.

domain have the potential to alter the antigenicity of ALK as they can modify its protein structure. To test the activity of the ALK vaccine against these mutants, we transduced ASB-XIV cells with a retroviral vector containing either the EML4-ALK WT or the EML4-ALK mutants (Fig. 7A). Control mice injected with ASB-XIV cells expressing the L1196M, C1156Y, or F1174L EML4-ALK mutants rapidly developed tumors in the lungs, whereas ALK vaccination almost completely prevented tumor growth of EML4-ALK WT and all mutants (Fig. 7B-E). Therefore, the ALK vaccine is not only efficacious against the EML4-ALK WT but also against some of the most common EML4-ALK mutants that develop in patients during treatment with crizotinib or ceritinib.

Discussion

In this work, we extended our previous findings on the efficacy of a DNA ALK vaccine against ALK-positive lymphoma to *ALK*-rearranged lung cancers. Compared with our previous work, we showed that the ALK vaccine is active not only in tumor grafts but also in primary *ALK*-rearranged NSCLC. Because the SP-C promoter is active since embryonic development (40), these mice are likely tolerant to human ALK. Thus, an important advance from

this work is the demonstration that an ALK vaccine can overcome tolerance in mice.

In addition, we showed that the ALK vaccine could be combined with either ALK TKI treatment or the anti-PD-1 antibody. These combinatorial therapies make the ALK vaccine attractive for potential clinical use. Current therapies for *ALK*-rearranged NSCLC, based on crizotinib or next-generation ALK TKIs, achieve a clinical response by arresting tumor progression or inducing tumor regression. However, all patients eventually relapse and die due to development of TKI resistance (11, 41).

In this work, we set the stage for the application of an ALK vaccine to further extend progression-free survival in NSCLC patients. The ALK vaccine induced a strong systemic and intratumoral immune response in mouse models of *ALK*-rearranged NSCLC, significantly reducing tumor growth and extending survival of treated mice, regardless of the type of *ALK* translocation (EML4-ALK or TFG-ALK). Simultaneous treatment during vaccination with crizotinib or TAE684 did not affect the ALK immune response achieved by the vaccine. Thus, these data indicate the feasibility of administering an ALK vaccine to NSCLC patients during ALK TKI treatment, possibly when the response is maximal in terms of tumor burden reduction.

Additional advantages of such a combination could stem from the potential activity of ALK TKIs in the regulation of the tumor immune microenvironment. We showed that the oncogenic activity of ALK directly regulated PD-L1 expression of the surface of tumor cells. High PD-L1 expression impaired the immune response against ALK elicited by the vaccine (Fig. 5). Therefore, PD-L1 downregulation by ALK TKI treatment could relieve the inhibitory feedback on intratumoral T cells and facilitate ALK-specific immune responses. Tumor cell death induced by ALK TKIs could release additional tumor neoantigens, including ALK itself, and thus enhance antitumor immune response (42, 43). Further investigation to elucidate the effect of ALK TKIs on the tumor microenvironment is required, but it is intriguing that studies in mouse models and metastatic melanoma patients showed an enhanced antitumor immune response after treatment with the selective B-RAF inhibitor (vemurafenib) alone, or in combination with MEK inhibitors (44, 45).

The immune microenvironment in *ALK*-rearranged tumors could therefore be a critical factor in the ALK-specific immune responses. We presented data indicating that *ALK*-rearranged mice indeed progressively develop an immunosuppressive tumor microenvironment similar to that induced in mice by oncogenic EGFR (34). Compared with WT mice, *ALK*-rearranged lungs accumulated higher numbers of PD-1⁺ T cells that also expressed the exhaustion markers TIM-3 and LAG-3, and showed increased numbers of tumor-infiltrating Tregs. *ALK*-rearranged NSCLC patients also showed a likely immunosuppressive microenvironment in the lungs with reduced tumor-infiltrating T cells.

In *ALK*-vaccinated lungs, the tumor-infiltrating Tregs were increased, and we detected a population of intratumoral CD8⁺ T cells with high expression of PD-1 (Supplementary Fig. S8A and S8B), which we interpreted as exhausted CD8⁺ T cells that had been elicited by the ALK vaccine to recognize the ALK antigen (46). In mice with advanced tumors, the ALK vaccine elicited a weaker ALK-specific cytotoxic response (Supplementary Fig. S8C) and decreased antitumor activity (Supplementary Fig. S2D). In these settings, Treg depletion by an antibody to CD25 could partially restore the impaired cytotoxic activity generated by the ALK vaccine (Supplementary Fig. S8C), indicating that Tregs could also play a critical role in the immunosuppressive tumor environment seen in *ALK*-rearranged lung tumors. Similarly, the restoration of the ALK vaccine efficacy by administration of antibody to PD-1 in high PD-L1 EML4-*ALK* ASB-XIV xenografts (Fig. 5) suggests that blockade of immune checkpoint molecules could powerfully potentiate the ALK vaccine.

Overall, these data suggest that combination therapy of ALK TKIs and ALK vaccine could work efficiently in the clinical setting to generate a strong and long-lasting immune response to ALK in NSCLC. The benefit from combined ALK TKI and ALK

vaccine therapy can be enhanced by additional immunotherapies, such as anti-PD-1/PD-L1 and anti-CTLA, to block immune checkpoints (17, 18) or through Treg depletion by antibodies to CD25 (47). Thus, the development of an ALK vaccine for clinical use, together with additional immunotherapeutic tools, provides exciting therapeutic options for the treatment of *ALK*-rearranged NSCLC.

Disclosure of Potential Conflicts of Interest

P.A. Jänne is a consultant/advisory board member for Chugai, Pfizer, and Roche. No potential conflicts of interest were disclosed by the other authors.

Authors' Contributions

Conception and design: C. Voena, G. Inghirami, R. Chiarle

Development of methodology: C. Voena, C. Mastini, F. Di Giacomo, C. Ambrogio, L. D'Amico, E. Panizza, R. Chiarle

Acquisition of data (provided animals, acquired and managed patients, provided facilities, etc.): C. Voena, M. Menotti, C. Mastini, F. Di Giacomo, D.L. Longo, B. Castella, M.E. BoggioMerlo, C. Ambrogio, V.G. Minero, T. Poggio, C. Martinengo, F. Cavallo, F. Altruda, M. Butaney, M. Capelletti, P.A. Jänne, R. Chiarle

Analysis and interpretation of data (e.g., statistical analysis, biostatistics, computational analysis): C. Voena, M. Menotti, C. Mastini, F. Di Giacomo, B. Castella, M.E. BoggioMerlo, C. Ambrogio, Q. Wang, V.G. Minero, C. Martinengo, M. Butaney, R. Chiarle

Writing, review, and/or revision of the manuscript: C. Voena, D.L. Longo, P.A. Jänne, R. Chiarle

Administrative, technical, or material support (i.e., reporting or organizing data, constructing databases): C. Voena, F. Cavallo, M. Butaney

Study supervision: R. Chiarle

Other (provided reagents): L. Mologni

Acknowledgments

The authors thank Glenn Dranoff for helpful discussions, Maria Stella Scalzo for technical support, Flavio Cristofani for housing and care of mice, Carlo Gambacorti-Passerini for kindly providing critical reagents, Silvio Aime for the Molecular Imaging Facility, and Sharmila Fagoonee and Maddalena Iannicella for technical help in generation of transgenic mice.

Grant Support

This work has been supported by grants FP7 ERC-2009-StG (proposal no. 242965—"Lunely") to R. Chiarle; Associazione Italiana per la Ricerca sul Cancro (AIRC) grant IG-12023 to R. Chiarle; Koch Institute/DFCC Bridge Project Fund to R. Chiarle; Ellison Foundation Boston to R. Chiarle; the Grant for Oncology Innovation by Merck-Serono to R. Chiarle; Worldwide Cancer Research (former AICR) grant 12-0216 to R. Chiarle; and R01 CA136851 to P.A. Jänne.

The costs of publication of this article were defrayed in part by the payment of page charges. This article must therefore be hereby marked *advertisement* in accordance with 18 U.S.C. Section 1734 solely to indicate this fact.

Received April 2, 2015; revised June 2, 2015; accepted July 23, 2015; published OnlineFirst September 29, 2015.

References

- Pao W, Girard N. New driver mutations in non-small-cell lung cancer. *Lancet Oncol* 2011;12:175–80.
- Berge EM, Doebele RC. Targeted therapies in non-small cell lung cancer: emerging oncogene targets following the success of epidermal growth factor receptor. *Semin Oncol* 2014;41:110–25.
- Soda M, Choi YL, Enomoto M, Takada S, Yamashita Y, Ishikawa S, et al. Identification of the transforming EML4-*ALK* fusion gene in non-small-cell lung cancer. *Nature* 2007;448:561–6.
- Chiarle R, Voena C, Ambrogio C, Piva R, Inghirami G. The anaplastic lymphoma kinase in the pathogenesis of cancer. *Nat Rev Cancer* 2008;8:11–23.
- Mano H. ALKoma: a cancer subtype with a shared target. *Cancer Discov* 2012;2:495–502.
- McDermott U, Iafrate AJ, Gray NS, Shioda T, Classon M, Maheswaran S, et al. Genomic alterations of anaplastic lymphoma kinase may sensitize tumors to anaplastic lymphoma kinase inhibitors. *Cancer Res* 2008;68:3389–95.

7. Kwak EL, Bang YJ, Camidge DR, Shaw AT, Solomon B, Maki RG, et al. Anaplastic lymphoma kinase inhibition in non-small-cell lung cancer. *N Engl J Med* 2010;363:1693–703.
8. Choi YL, Soda M, Yamashita Y, Ueno T, Takashima J, Nakajima T, et al. EML4-ALK mutations in lung cancer that confer resistance to ALK inhibitors. *N Engl J Med* 2010;363:1734–9.
9. Shaw AT, Kim DW, Nakagawa K, Seto T, Crino L, Ahn MJ, et al. Crizotinib versus chemotherapy in advanced ALK-positive lung cancer. *N Engl J Med* 2013;368:2385–94.
10. Solomon B, Wilner KD, Shaw AT. Current status of targeted therapy for anaplastic lymphoma kinase-rearranged non-small cell lung cancer. *Clin Pharmacol Ther* 2014;95:15–23.
11. Shaw AT, Kim DW, Mehra R, Tan DS, Felip E, Chow LQ, et al. Ceritinib in ALK-rearranged non-small-cell lung cancer. *N Engl J Med* 2014;370:1189–97.
12. Friboulet L, Li N, Katayama R, Lee CC, Gainor JF, Crystal AS, et al. The ALK inhibitor ceritinib overcomes crizotinib resistance in non-small cell lung cancer. *Cancer Discov* 2014;4:662–73.
13. Katayama R, Shaw AT, Khan TM, Mino-Kenudson M, Solomon BJ, Halmos B, et al. Mechanisms of acquired crizotinib resistance in ALK-rearranged lung cancers. *Sci Transl Med* 2012;4:120ra17.
14. Lovly CM, McDonald NT, Chen H, Ortiz-Cuaran S, Heukamp LC, Yan Y, et al. Rationale for co-targeting IGF-1R and ALK in ALK fusion-positive lung cancer. *Nat Med* 2014;20:1027–34.
15. Doebele RC, Pilling AB, Aisner DL, Kutateladze TG, Le AT, Weickhardt AJ, et al. Mechanisms of resistance to crizotinib in patients with ALK gene rearranged non-small cell lung cancer. *Clin Cancer Res* 2012;18:1472–82.
16. Voena C, Di Giacomo F, Panizza E, D'Amico L, Boccalatte FE, Pellegrino E, et al. The EGFR family members sustain the neoplastic phenotype of ALK+ lung adenocarcinoma via EGFR1. *Oncogenesis* 2013;2:e43.
17. Topalian SL, Hodi FS, Brahmer JR, Gettinger SN, Smith DC, McDermott DF, et al. Safety, activity, and immune correlates of anti-PD-1 antibody in cancer. *N Engl J Med* 2012;366:2443–54.
18. Brahmer JR, Tykodi SS, Chow LQ, Hwu WJ, Topalian SL, Hwu P, et al. Safety and activity of anti-PD-L1 antibody in patients with advanced cancer. *N Engl J Med* 2012;366:2455–65.
19. Chiarle R, Martinengo C, Mastini C, Ambrogio C, D'Escamard V, Forni G, et al. The anaplastic lymphoma kinase is an effective oncoantigen for lymphoma vaccination. *Nat Med* 2008;14:676–80.
20. Pulford K, Falini B, Banham AH, Codrington D, Robertson H, Hatton C, et al. Immune response to the ALK oncogenic tyrosine kinase in patients with anaplastic large-cell lymphoma. *Blood* 2000;96:1605–7.
21. Passoni L, Scardino A, Bertazzoli C, Gallo B, Coluccia AM, Lemonnier FA, et al. ALK as a novel lymphoma-associated tumor antigen: identification of 2 HLA-A2.1-restricted CD8+ T-cell epitopes. *Blood* 2002;99:2100–6.
22. Ait-Tahar K, Cerundolo V, Banham AH, Hatton C, Blanchard T, Kusec R, et al. B and CTL responses to the ALK protein in patients with ALK-positive ALCL. *Int J Cancer* 2006;118:688–95.
23. Ait-Tahar K, Barnardo MC, Pulford K. CD4 T-helper responses to the anaplastic lymphoma kinase (ALK) protein in patients with ALK-positive anaplastic large-cell lymphoma. *Cancer Res* 2007;67:1898–901.
24. Passoni L, Gallo B, Biganzoli E, Stefanoni R, Massimino M, Di Nicola M, et al. In vivo T-cell immune response against anaplastic lymphoma kinase in patients with anaplastic large cell lymphomas. *Haematologica* 2006;91:48–55.
25. Ait-Tahar K, Damm-Welk C, Burkhardt B, Zimmermann M, Klapper W, Reiter A, et al. Correlation of the autoantibody response to the ALK oncoantigen in pediatric anaplastic lymphoma kinase-positive anaplastic large cell lymphoma with tumor dissemination and relapse risk. *Blood* 2010;115:3314–9.
26. Guerra C, Mijimolle N, Dhawahir A, Dubus P, Barradas M, Serrano M, et al. Tumor induction by an endogenous K-ras oncogene is highly dependent on cellular context. *Cancer Cell* 2003;4:111–20.
27. Politi K, Zakowski MF, Fan PD, Schonfeld EA, Pao W, Varmus HE. Lung adenocarcinomas induced in mice by mutant EGF receptors found in human lung cancers respond to a tyrosine kinase inhibitor or to down-regulation of the receptors. *Genes Dev* 2006;20:1496–510.
28. Kim H, Jang SJ, Chung DH, Yoo SB, Sun P, Jin Y, et al. A comprehensive comparative analysis of the histomorphological features of ALK-rearranged lung adenocarcinoma based on driver oncogene mutations: frequent expression of epithelial-mesenchymal transition markers than other genotype. *PLoS One* 2013;8:e76999.
29. Soda M, Takada S, Takeuchi K, Choi YL, Enomoto M, Ueno T, et al. A mouse model for EML4-ALK-positive lung cancer. *Proc Natl Acad Sci U S A* 2008;105:19893–7.
30. Ambrogio C, Carmona FJ, Vidal A, Falcone M, Nieto P, Romero OA, et al. Modeling lung cancer evolution and preclinical response by orthotopic mouse allografts. *Cancer Res* 2014;74:5978–88.
31. Chen Z, Sasaki T, Tan X, Carretero J, Shimamura T, Li D, et al. Inhibition of ALK, PI3K/MEK, and HSP90 in murine lung adenocarcinoma induced by EML4-ALK fusion oncogene. *Cancer Res* 2010;70:9827–36.
32. Quakkelaar ED, Melief CJ. Experience with synthetic vaccines for cancer and persistent virus infections in nonhuman primates and patients. *Adv Immunol* 2012;114:77–106.
33. Jacob JB, Quaglino E, Radkevich-Brown O, Jones RF, Piechocki MP, Reyes JD, et al. Combining human and rat sequences in her-2 DNA vaccines blunts immune tolerance and drives antitumor immunity. *Cancer Res* 2010;70:119–28.
34. Akbay EA, Koyama S, Carretero J, Altabel A, Tchaicha JH, Christensen CL, et al. Activation of the PD-1 pathway contributes to immune escape in EGFR-driven lung tumors. *Cancer Discov* 2013;3:1355–63.
35. Ota K, Azuma K, Kawahara A, Hattori S, Iwama E, Tanizaki J, et al. Induction of PD-L1 expression by the EML4-ALK oncoprotein and downstream signaling pathways in non-small cell lung cancer. *Clin Cancer Res* 2015;21:4014–21.
36. Peggs KS, Quezada SA, Allison JP. Cell intrinsic mechanisms of T-cell inhibition and application to cancer therapy. *Immunol Rev* 2008;224:141–65.
37. Herbst RS, Soria JC, Kowanetz M, Fine GD, Hamid O, Gordon MS, et al. Predictive correlates of response to the anti-PD-L1 antibody MPDL3280A in cancer patients. *Nature* 2014;515:563–7.
38. Garon EB, Rizvi NA, Hui R, Leigh N, Balmanoukian AS, Eder JP, et al. Pembrolizumab for the treatment of non-small-cell lung cancer. *N Engl J Med* 2015;372:2018–28.
39. Shaw AT, Engelman JA. ALK in lung cancer: past, present, and future. *J Clin Oncol* 2013;31:1105–11.
40. Frederick DT, Piris A, Cogdill AP, Cooper ZA, Lezcano C, Ferrone CR, et al. BRAF inhibition is associated with enhanced melanoma antigen expression and a more favorable tumor microenvironment in patients with metastatic melanoma. *Clin Cancer Res* 2013;19:1225–31.
41. Simonet WS, DeRose ML, Bucay N, Nguyen HQ, Wert SE, Zhou L, et al. Pulmonary malformation in transgenic mice expressing human keratinocyte growth factor in the lung. *Proc Natl Acad Sci U S A* 1995;92:12461–5.
42. Shaw AT, Engelman JA. Ceritinib in ALK-rearranged non-small-cell lung cancer. *N Engl J Med* 2014;370:2537–9.
43. Vanneman M, Dranoff G. Combining immunotherapy and targeted therapies in cancer treatment. *Nat Rev Cancer* 2012;12:237–51.
44. Kroemer G, Galluzzi L, Kepp O, Zitvogel L. Immunogenic cell death in cancer therapy. *Annu Rev Immunol* 2013;31:51–72.
45. Knight DA, Ngjow SF, Li M, Parmenter T, Mok S, Cass A, et al. Host immunity contributes to the anti-melanoma activity of BRAF inhibitors. *J Clin Invest* 2013;123:1371–81.
46. Yadav M, Jhunjhunwala S, Phung QT, Lupardus P, Tanguay J, Bumbaca S, et al. Predicting immunogenic tumour mutations by combining mass spectrometry and exome sequencing. *Nature* 2014;515:572–6.
47. Rech AJ, Mick R, Martin S, Recio A, Aqui NA, Powell DJ Jr., et al. CD25 blockade depletes and selectively reprograms regulatory T cells in concert with immunotherapy in cancer patients. *Sci Transl Med* 2012;4:134ra62.

Cancer Immunology Research

Efficacy of a Cancer Vaccine against *ALK*-Rearranged Lung Tumors

Claudia Voena, Matteo Menotti, Cristina Mastini, et al.

Cancer Immunol Res 2015;3:1333-1343. Published OnlineFirst September 29, 2015.

Updated version Access the most recent version of this article at:
doi:[10.1158/2326-6066.CIR-15-0089](https://doi.org/10.1158/2326-6066.CIR-15-0089)

Supplementary Material Access the most recent supplemental material at:
<http://cancerimmunolres.aacrjournals.org/content/suppl/2015/10/17/2326-6066.CIR-15-0089.DC1>

Cited articles This article cites 47 articles, 21 of which you can access for free at:
<http://cancerimmunolres.aacrjournals.org/content/3/12/1333.full#ref-list-1>

E-mail alerts [Sign up to receive free email-alerts](#) related to this article or journal.

Reprints and Subscriptions To order reprints of this article or to subscribe to the journal, contact the AACR Publications Department at pubs@aacr.org.

Permissions To request permission to re-use all or part of this article, use this link
<http://cancerimmunolres.aacrjournals.org/content/3/12/1333>.
Click on "Request Permissions" which will take you to the Copyright Clearance Center's (CCC) Rightslink site.